

The VLT-VIRMOS Mask Manufacturing Unit

G. CONTI, E. MATTAINI, L. CHIAPPETTI, D. MACCAGNI, E. SANT'AMBROGIO, D. BOTTINI, AND B. GARILLI

CNR, Istituto di Fisica Cosmica "G. Occhialini," via Bassini 15, I-20133 Milano, Italy; conti@ifctr.mi.cnr.it

O. LE FÈVRE, M. SAISSE, AND C. VOËT

Laboratoire d'Astrophysique de Marseille, Traverse du Siphon, F-13376 Marseille, France; Olivier.LeFevre@astrsp-mrs.fr

O. CAPUTI, E. CASCONI, D. MANCINI, G. MANCINI, F. PERROTTA, AND P. SCHIPANI

Osservatorio Astronomico di Capodimonte, via Moiariello 16, I-80131 Napoli, Italy; mancini@cerere.na.astro.it

AND

G. VETTOLANI

CNR, Istituto di Radioastronomia, via Gobetti 101, I-40129 Bologna, Italy; vettolani@ira.bo.cnr.it

Received 2000 December 5; accepted 2001 January 12

ABSTRACT. The VIRMOS Consortium had the task to design and manufacture two spectrographs for the ESO Very Large Telescope, VIMOS (Visible Multi-Object Spectrograph) and NIRMOS (Near Infrared Multi-Object Spectrograph). This paper describes how the mask manufacturing unit (MMU), which cuts the slit masks to be used with both instruments, meets the scientific requirements and manages the storage and the insertion of the masks into the instrument. The components and the software of the two main parts of the MMU, the mask manufacturing machine and the mask handling system, are illustrated together with the mask material and with the slit properties. Slit positioning is accurate within $15\ \mu\text{m}$, equivalent to $0''.03$ on the sky, while the slit edge roughness has an rms on the order of 0.03 pixels on scales of a slit $5''$ long and of 0.01 pixels on the pixel scale ($0''.205$). The MMU was successfully installed during 2000 July/August at the Paranal Observatory and is now operational for spectroscopic mask cutting, in compliance with the requested specifications.

1. INTRODUCTION

The VIRMOS (Visible and Infrared Multi-Object Spectrographs) project is the response by a French-Italian Consortium of astronomical institutes to the ESO request for two spectrographs with enhanced survey capabilities to be installed at the Very Large Telescope (VLT). It consists of the twin instruments VIMOS (Visible Multi-Object Spectrograph) and NIRMOS (Near Infrared Multi-Object Spectrograph), with a large field of view split into four quadrants and a high multiplexing factor in their multiobject spectroscopy (MOS) observing modes (Le Fèvre et al. 1998, 2000). VIMOS is going to be offered to the European astronomical community starting 2001 July at VLT-UT3, and NIRMOS is expected to be operational at the end of 2002 at VLT-UT4. In MOS mode, both instruments make use of slit masks which the astronomer can design following the observational requirements. Thus, the VIRMOS project includes the delivery to ESO of a complete, independent, off-line facility to manufacture and handle the masks needed by the two spectrographs.

Multiobject spectrographs currently operational or forthcoming at other telescopes have adopted machining solutions ranging from laser punching to milling machines and either aluminum or carbon fiber as masks: the MOS/OSIS instrument at

the Canada-France Hawaii-Telescope uses $75\ \mu\text{m}$ thick black anodized aluminum masks cut by a laser machine (Di Biagio, Le Coarer, & Lemaitre 1990); at the KECK telescopes the LRIS instrument uses mechanically punched 0.4 mm thick aluminum masks (Oke et al. 1995), while the DEIMOS instrument¹ will use 0.25 mm masks prepared by a milling machine; the GMOS spectrograph for the Gemini telescopes uses 0.2 mm thick carbon fiber masks cut by a laser machine (Szeto et al. 1997).

In the VIMOS case we selected the laser technique to cut the masks in 0.2 mm thick invar sheets. In this paper, we will describe our mask manufacturing unit (MMU), which has been operational at the Paranal Observatory since 2000 August. The MMU is presently used to provide the instrument FORS2 with the masks to be used in its mask exchange unit (MXU) (Schink et al. 2000) and will be used with VIMOS when it arrives in Paranal in early 2001. In § 2 we illustrate the requirements and specifications the MMU had to satisfy and in § 3 the adopted hardware configurations. Sections 4 and 5 respectively describe the tests and tuning of the mask manufacturing machine (MMM) and the resulting performances. Finally, § 6 outlines the MMU operational concepts.

¹ <http://www.ucolick.org/~phillips/deimos/masks.html>.

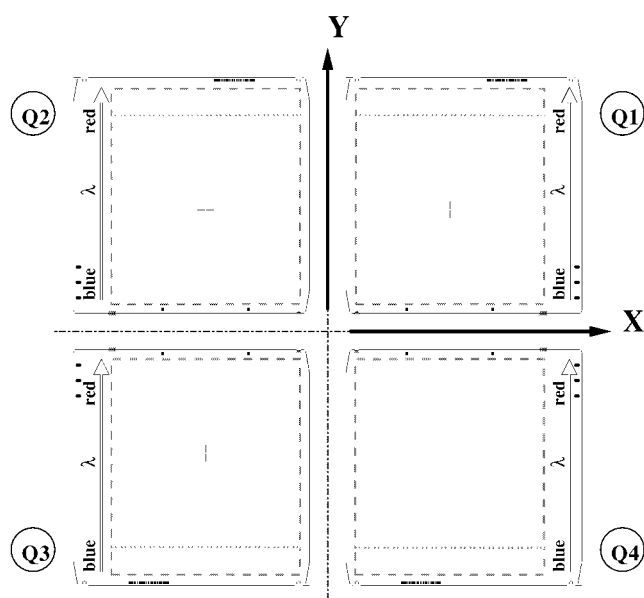


FIG. 1.—Location in the four VIMOS quadrants of the four masks with all contours and other details (see Fig. 3) and respective orientation in the common reference system (which is oriented as the MMM reference system). The dispersion direction of the spectra is also indicated. The cross marks the position of the optical axis (which is not coincident with the mask center), while the dashed line indicates the 244×279 mm “useful area” corresponding to the detector field of view. The dotted line delimits a square 244×244 mm area around the optical axis.

2. MMU REQUIREMENTS AND SPECIFICATIONS

2.1. Masks

The VIMOS (and NIRMOS) focal plane is divided into four quadrants, therefore four masks (one mask set) are needed for every MOS observation. The scale at the focal plane where masks must be inserted is $0.578 \text{ mm arcsec}^{-1}$, and each quadrant has a field of view of $7' \times 8'$ ($8' \times 6'$ NIRMOS). This defines the gross dimensions of the masks and, together with the expected best seeing at the VLT ($\sim 0''.3$), the minimum slit width. Although the VLT Nasmyth focal plane has a curvature radius of 2 m, the VIMOS focal-plane adaptation lens brings this radius to 4 m, and the tilting of the quadrants’ optical axes by $\sim 2^\circ$ makes possible the use flat masks with a maximum allowed thickness of 0.4 mm. Figure 1 shows an outline of the VIMOS focal plane with its reference system. The size of the masks is 305×305 mm, and the contour geometry is determined by the mechanical interface with the focal plane and with the automatic mask insertion mechanism.

The number of slits in each mask can be more than 200, depending on slit length and spectral coverage. The highest multiplexing factor can be attained by observing with the low-resolution ($R \sim 200$) VIMOS grisms, when up to five rows of spectra can be stacked on each CCD. Typical slits are rectan-

gular with width $\geq 200 \mu\text{m}$ ($0''.35$), but the possibility to cut also curved slits must be supported.

The roughness of the slit edges must be as low as possible on spatial scales between the detector pixel size (0.12 mm at the focal plane for VIMOS) and the slit length (typically 6 mm, equivalent to $10''$), to optimize sky subtraction in spectroscopic data reduction. This specification has been quantified as follows: the rms roughness at pixel-size scales must be $\leq 2 \mu\text{m}$, and the slit edge waviness must be $\leq 3 \mu\text{m}$. The slit edge roughness shall be regularly inspected to verify the machine performances.

The mask cutting speed shall be sufficient to allow the production of the masks for eight observing fields (32 masks) in an 8 hour work shift (15 minutes per mask). For a typical 200 slit mask the total length to be cut is about 4500 mm (including the overhead for the mechanical interface); therefore the requirement translates in a cutting speed $\geq 6 \text{ mm s}^{-1}$.

One of the most critical items is the slit positioning accuracy in the focal plane, which eventually determines whether the chosen set of objects are going to be found in the slits when pointing the telescope. The error budget is made of several components: (1) the mapping accuracy of the CCD onto the focal plane, i.e., the accuracy with which optical distortions are taken into account; (2) the mask scale variations, i.e., the thermal expansion of the mask material due to the temperature variations between mask manufacturing and spectroscopic observation; (3) the positioning accuracy of the slit cutting machine; and (4) the accuracy of the positioning of the mask in the focal plane and its repeatability. The overall acceptable positioning accuracy is $\frac{1}{3}$ of a pixel (slits of $1''$ width project onto 5 pixels), which means $\leq 30 \mu\text{m}$. Component 1 contributes $3 \mu\text{m}$, the rms of the fit of the transformation matrix from pixels to millimeters in the focal plane; component 4 is estimated to be $\sim 10 \mu\text{m}$, since the mask contours can be customized to the as-built focal-plane mechanical interface. Thus, $\sim 17 \mu\text{m}$ are allowed for components 2 and 3.

The mask surfaces shall have the lowest possible reflectivity at the operating wavelengths (370–1850 nm).

2.2. Mask Handling

To minimize observing overheads and to avoid having people inside the domes during the night, MOS instruments at the VLT must be able to change the mask configuration through remote control: in our case, both VIMOS and NIRMOS can have 15 different mask sets at any time. For each instrument and for each quadrant there is a demountable instrument cabinet (IC) that must be prepared by the MMU operator by inserting the requested masks as much in advance of the spectroscopic observations as possible. These requirements imply that a large number of masks is kept available at any time, from which the ones to be inserted in the ICs for the following night(s) of observation are chosen. Storage for 100 mask sets (400 masks) has to be provided. The masks must thus be uniquely identified and must be traceable, and their position in each IC must be

TABLE 1
LASER CUTTING MACHINE CHARACTERISTICS

Item	Description
Manufacturer	LPKF Laser & Electronics AG, Garbsen (Germany)
Model	StencilLaser System 600/600
Stand	Natural granite
Cutting area	600 × 600 mm
XY motion	DC servo-motors + rotary encoders, resolution 0.5 μm
XY motion calibration	Glass linear rules, resolution 0.5 μm
Working platform	Supported by four air pads on the granite stand
XY accuracy on full travel	± 10 μm
Repeat accuracy	3 μm
XY squareness	<5"
Laser cut location accuracy	≤15 μm
Laser cut dimensions repeatability	± 2 μm
Cutting speed range	1–50 mm s ⁻¹
Laser head	Flashlamp pumped Nd:YAG (1064 nm) Maximum power 60 W Lamp life ~400 hr Maximum pulse rate 4000 Hz
Laser beam diameter	40 μm
Gas for cutting assist	Air 16 bar
Water cooling	External chiller
Gas exhausting system	Yes
Realignment after lamps changing	No
Laser safety (normal operation)	Class 1 laser product
Control	PC via RS232
Overall dimensions	1750 × 2300 × 1350 mm
Dimensions of control rack	600 × 950 × 1900 mm
Total weight	~3000 kg
Software	CircuitCam to generate proprietary format files StencilMaster to control the cutting operations

certain and made known to the instrument control software. A mask handling system, providing hardware and software tools to reach the goal of having the right mask in the focal plane at the right time, must be implemented.

3. ADOPTED SOLUTIONS AND MMU CONFIGURATION

3.1. Short History

In the initial concept (1997), the MMM was intended as a milling machine which would cut the slits in a 0.1 mm thin brass sheet, supported by a 10 mm thick aluminum frame. We assembled a small milling machine, and we proved that the roughness and speed requirements could be fulfilled. The minimum obtainable slit width was 300 μm. This solution was discarded because the ICs were too large and the accuracy in the slit positioning was hampered by the thermal expansion of brass, given the possible temperature differences between the time a mask was manufactured and used in the instrument or the temperature variations during the observations. Furthermore, the lifetime of the cutting tools was short because of breaking and wear (which caused a slit width variation). Subsequent developments (1998) were aimed at minimizing the sources of errors, by making use of aluminum and thicker (but still less than 0.3 mm), frameless masks, which had the ad-

vantage of reducing the size and the weight of the ICs. The next natural step was the use of a material with a low thermal expansion coefficient: we tested carbon fiber, kevlar, graphite, and invar, but it was impossible to obtain the required slit edge quality with a milling machine. Only recently has a new type of laser cutting machine, called StencilLaser, become available on the market. In particular, one machine could meet the specifications by making use of 0.2 mm thick invar sheets. The cutting speed makes it possible to cut the mask contour on the machine itself; thus the masks can be frameless and customized to the quadrant interface where it will have to be mounted, and, as a further bonus, also any slit width ≥80 μm became a possibility. For a full account of the trade-off between the two solutions (milling and laser cutting) and for the choice of the laser machine manufacturer, see Conti et al. (1999).

3.2. The Mask Manufacturing Machine

Our choice for the MMM was the StencilLaser 600 by LPKF, whose main characteristics are given in Table 1. The machine uses a pulsed Nd:YAG laser head that, for normal operation, is classified for safety as a class 1 laser product (as safe as a compact disc player). The laser head is fixed while the working platform, on which the invar sheet is mounted, is moved in XY by two servo-motors over four air pads. Cutting occurs under



FIG. 2.—LPKF laser cutting machine installed in Milano. An invar sheet is mounted and clamped on the working platform. For mask cutting, the laser focusing system moves down close to the sheet and the whole platform is displaced in the X and Y directions.

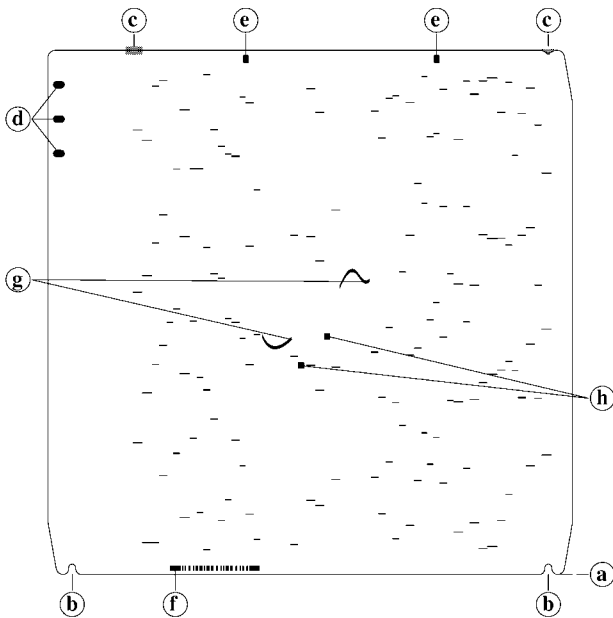


FIG. 3.—Layout of typical VIMOS mask (quadrant 3) showing contour and slits and the following features: (a) the cutting of the contour starts outside the mask area to have a clean outline; (b) the two bottom notches are used to position the mask inside the IC; (c) the two upper notches (*in gray*), a rectangular one and a triangular one, make the reference for mask positioning in the focal plane: they are cut with the same accuracy as the slits; (d) the three oval holes are the grabbing points of the clamp for moving the mask from the IC to the focal plane and back; (e) the two rectangular fixing holes are used to hold the mask in position in focal plane; (f) the six-digit bar code used to identify the mask; (g) two curved slits; and (h) two square slits corresponding to the positions of two reference objects used for fine alignment of the mask on the sky.

a 16 bar compressed air jet. The whole cutting process is controlled by the LPKF StencilMaster software running on a PC called the mask manufacturing control unit (MMCU). A picture of the machine can be seen in Figure 2.

3.3. The Mask Material and the Raw Mask Preparation

The chosen mask material is invar, a 36%Ni-64%Fe alloy² with a thickness of 0.2 mm. The main mechanical and thermal characteristics of invar compared with aluminum and stainless steel are given in Table 2.

Mask manufacturing includes, as a last operation, the cutting of the contour; therefore the raw invar sheets shall have larger dimensions than the masks, to fix them on the working platform of the laser cutting machine. We adopted 450×340 mm sheets that weigh 0.250 kg each.

The yearly mask need for VIMOS is estimated to be ~ 2000 . One aim of our work was to find a method to prepare a large quantity of raw masks at the lowest cost. Invar is delivered in rolls at the requested width and must be coated with a black antireflection paint. The requested characteristics for the coating are thickness less than $20 \mu\text{m}$; good adhesion to the metallic substrate; dull black color; uniformity of the coating over the two surfaces. The adopted procedure³ for the raw mask preparation consists of chemical and mechanical cleaning; black coating of the two sides of the strip, using a roller system; warm curing of the varnish; insertion of a low adhesion plastic protective film; straightening and destressing to eliminate the roll curvature; cutting to the requested dimensions; visual inspection for absence of wrinkles and scratches; packing in folders of 20 sheets each. This industrial procedure has the disadvantage that the first and last parts of the strip must be discarded because of mechanical damage. For a 450 mm wide strip this loss can be quantified as about 100 kg of material. However, we obtained 4400 sheets out of 1200 kg of invar, at a cost of ~ 11 DM per sheet. Figure 3 shows a typical VIMOS mask.

Measurements of the specular and diffuse reflectance of coated invar samples at 633 and 1150 nm give the results shown in Table 3.

3.4. The Mask Handling System

The concept of the mask handling system (MHS) is to provide the hardware and software necessary to control the mask flow.

Mask identification is done by direct cutting of a six-digit bar code at 3 mm from the edge of the masks using the European standard 2/5 Interleaved Code (EN 801). The most significant digit of the code identifies the quadrant (from 1 to 4 for VIMOS and from 5 to 8 for NIRMOS). Two bar code scanners⁴ provide the decoding during all the operations of the MHS. All masks that, at a given time, are not inserted into the

² By Krupp VDM, Werdohl, Germany; trade name Pernifer 36.

³ Implemented by CEM Lavorazioni Elettrochimiche srl, Milano, Italy.

⁴ Datalogic, Bologna, Italy; model DS2100-1000.

TABLE 2
COMPARISON OF INVAR CHARACTERISTICS

Characteristic	Invar	Al	Steel
Coefficient of thermal expansion ($10^{-6} \text{ }^{\circ}\text{C}^{-1}$)	0.8	23	9.5
Modulus of elasticity (10^9 N m^{-2})	143	69	200
Density (10^3 kg m^{-3})	8.1	2.7	8
Specific stiffness ($10^6 \text{ m}^2 \text{ s}^{-2}$)	18	26	25

ICs are stored in the storage cabinet (SC) of the relative instrument.

Figure 4 shows a picture of the in-house-manufactured VIMOS SC. It can store 400 masks (100 mask sets) inserted vertically into transparent polycarbonate slots in such a way that the bar code can be read by the scanner mounted on a sliding stage. Because of the space constraint, the VIMOS SC has two quadrants per side, and the bar code scanner must be moved from one side to the other with the connection cable suspended on the ceiling by a rotating pivot.

The 15 masks in each IC (which is part of the instrument and not of the MMU) are packed with a pitch of 4.5 mm. Before observations the ICs must be prepared by unloading

TABLE 3
COATED INVAR REFLECTANCE

Wavelength (nm)	Specular Reflectance (%)	Diffuse Reflectance (%)
633	0.04	4.7
1150	0.04	3.7

the masks no longer necessary and loading the requested new ones. This operation is quite delicate because a mask in a wrong IC or in a wrong slot in the IC will jeopardize the observation. Mask insertion is thus controlled by a robot,⁵ shown in Figure 5, that performs a software-controlled Z displacement. The four ICs are mounted in fixed order (constrained by the mechanical interfaces) into an IC box that is placed on the robot platform. The robot moves it with an accuracy of about 0.1 mm, in order to place the appropriate IC slot in front of a mask stand (see Fig. 5). The Z positions of the slots are calibrated and stored in a table used by the software to command the robot displac-

⁵ Produced by ANTIL srl, S. Giuliano Milanese, Italy.

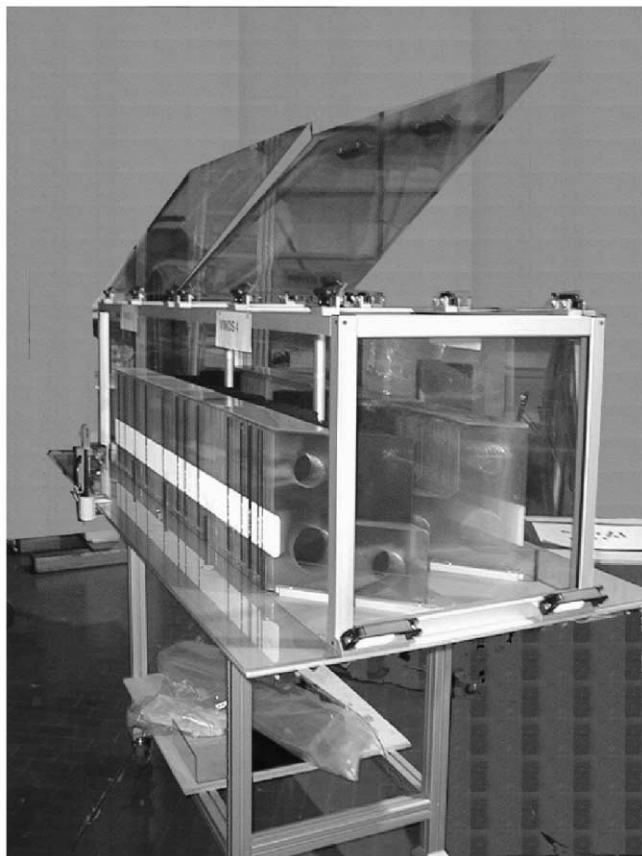


FIG. 4.—VIMOS storage cabinet. The white surfaces are used as background for the bar code during mask identification.



FIG. 5.—The VIMOS instrument cabinet robot with the empty IC box placed on its platform and a mask positioned on the stand.

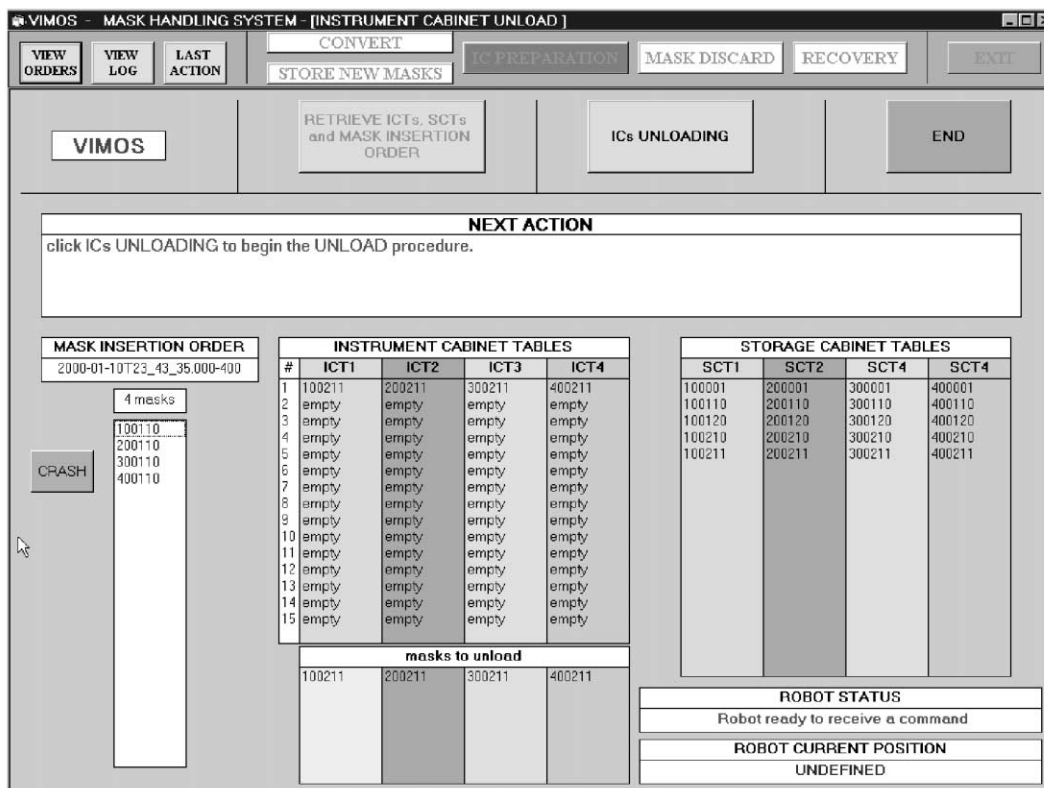


Fig. 6.—Example of a GUI of the MHSw (IC preparation/unload [sub]function)

ment. Then the unloading/loading operation is done manually by means of a moving clamp, with the assistance of a bar code scanner identical to the one used in the SC. This bar code scanner is also used for off-line mask identification (storage after manufacturing).

The third part of the MHS is the mask handling control unit (MHCU), a PC that runs the mask handling software (MHSw) and the LPKF CircuitCam software and connects the bar code scanners and the IC robot.

3.5. Software Components

The MMU software components developed in-house to support the operational procedures described in § 6 are as follows:

1. The MHSw running on MHCU, which provides a graphical user interface (GUI) (see Fig. 6) for all mask handling functions except the actual manufacturing, records where masks are stored, handles the communication with instrument/VLT software, and acts as a front end to the LPKF CircuitCam software (see § 6.1).

2. The Cut Manager software running on MMCU is a simple GUI which assists orderly usage (and archiving) of mask files and acts as a front end to LPKF StencilMaster, used to cut the masks.

3. A mirroring module that runs on both computers to keep synchronized the various data files on the disks, allowing easy recovery in the case of a failure of one.

All software is developed using Microsoft Visual Basic 6.0 under Windows NT operating system.

3.6. The Quality Control Equipment

The cutting performance of the laser machine from the point of view of the slit edge roughness must be periodically controlled to be within the specifications reported in § 2.1. We have defined the following quality control procedure: nine square samples (30 mm side) are cut from an invar sheet under the same laser machine settings as the mask slits. The roughness of the sample borders is measured by a mechanical roughness meter.⁶ The samples are placed vertically under the measuring probe, which is a 1 mm wide chisel edge stylus with 5 μm tip radius, which measures the roughness over the full thickness of the 0.2 mm samples. The roughness can be due to both the laser cutting process itself and the residual invar melting flashes. The instrument is connected to a third PC where all measurements carried out during the lifetime of the MMU can

⁶ Taylor Hobson, Ltd., Leicester, UK; model Talysurf Plus.

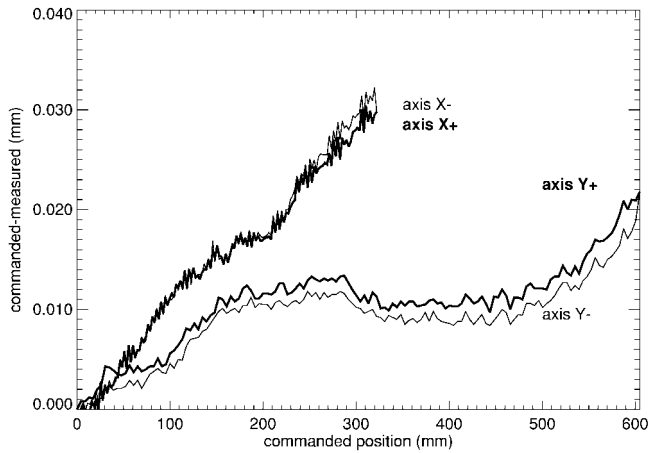


FIG. 7.—Content of a typical laser machine calibration file obtained on 2000 May 8. The abscissa of the plot corresponds to a commanded excursion on the X or Y axis of the machine (for our application we use the whole X excursion but only the central part of the Y excursion). The calibration procedure records the difference between the requested position and the actual position measured by the linear glass rules (this difference is shown in ordinate) once moving in the forward (positive) direction (*thick line*) and once in the backward (negative) direction (*thin line*). The difference between the two curves gives an indication of the backlash of the motion system. Actual movements during cutting are compensated for using the content of the calibration file (by default the positive direction curve is used).

be acquired, analyzed, and archived. The slit width is checked by a microscope with a calibrated reticle.

4. TEST AND TUNING OF THE LASER CUTTING MACHINE

4.1. Performance Verification

The StencilMaster software by LPKF controls the whole cutting process, i.e., the displacement of the working platform and the laser parameter settings and switching. The XY motion system is controlled by rotary encoders on the motor shafts, but a calibration of the system itself can be done using the linear glass rules provided on the two axes. During such procedure the working platform moves, backward and forward, along the Y and X directions, with a predefined step to cover the whole traveling range. After each step the displacement is read on the rules, and the difference between the requested and actual positions is stored in a calibration file. During normal cutting operation such correction is applied to the requested position to take into account this difference. A new calibration of the motion system is recommended if a significant temperature variation occurs or if the machine is switched off for some days. A typical calibration file is plotted in Figure 7.

To verify the accuracy of the working platform displacements after calibration, we used a laser interferometer system⁷ with a resolution of $0.1 \mu\text{m}$ and an accuracy of ± 0.5 ppm. Normally

TABLE 4
LASER MACHINE TOOL SETTINGS

Parameter	"Cutting Fine"	"Cutting"
Cutting speed (mm s^{-1})	6	20
Laser power (W)	19	21
Voltage (V)	235	269
Laser pulse frequency (Hz)	1200	1600
Laser pulse width (ms)	0.19	0.11

the readings from the internal linear glass rules are not accessible while the machine is moving. For this reason a single (uncalibrated) step displacement was commanded manually, and, when done, the internal rule reading was recorded together with the interferometer displacement measurement. The agreement between the two measures was within $\pm 2 \mu\text{m}$, which confirms the accuracy of the LPKF machine displacements. We did further tests asking for selected linear cuts along the interferometer beam (alternately mounted along X and Y) and reading the interferometer readout and the glass rules at the starting and ending positions. We have verified that during cutting the movements are commanded in calibrated units, with the expected accuracy.

The laser beam correctly focused has a diameter of $40 \mu\text{m}$. The CircuitCam program that calculates the cutting paths takes into account this value to obtain the requested slit dimensions. The slit width measurements show an error of $\pm 2 \mu\text{m}$, independently of the slit width.

4.2. Cutting Tool Tuning

The file describing each mask (see § 6.1) contains the mask slit pattern, the bar code, the other features, and the appropriate quadrant contour associated with different "layers." To each layer corresponds a cutting tool, i.e., a particular cutting speed and laser setup parameters. Among several possible choices, we carried out a series of tests to find the best tool (called the "cutting fine") that would satisfy the edge roughness specifications while working at the necessary speed, while a faster but rougher "cutting" tool is used for contour and lower precision features. Table 4 gives the adopted tool settings.

The speed and frequency are fixed parameters while the others are adjusted at each laser lamp change to keep the power constant. The best focus of the laser beam must be positioned inside the thickness of the cutting material. It can be adjusted by a micrometer that determines the distance of the focusing lens from the sheet during cutting; we have verified that also this parameter influences the edge roughness, and we have optimized it (this tuning has been repeated after the installation in Paranal).

5. RESULTING PERFORMANCES

5.1. Mask Cutting Time

The time needed for mask manufacturing includes a fixed overhead of about 460 s for invar sheet mounting operations,

⁷ Hewlett Packard model 5526A.

TABLE 5
SLIT EDGE ROUGHNESS

Parameter	Measured (μm)	Required (μm)
W_q (cutoff = 0.12 mm)	0.35 ± 0.08	≤ 2
W_r (cutoff = 2.5 mm)	1.06 ± 0.43	≤ 3

connection setup, bar code and contour cutting and scales up to 950 s for a mask with 200 slits. Thus, at most two 8 hour shifts are necessary to cut the 60 masks which would fill the four ICs of one instrument.

5.2. Slit Positioning Accuracy

Having made allowance for the accuracy of the CCD mapping onto the focal plane and for the repeatability of the mask positioning in the focal plane (see § 2.1), we must verify that the invar thermal expansion and the positioning accuracy of the laser machine allow us to place slits within $17 \mu\text{m}$. Mask manufacturing occurs at a controlled temperature of 20°C while the average temperature at Paranal is 10°C ; thus the (negative) invar expansion over the mask size is only $\sim 2 \mu\text{m}$.

To verify the real accuracy of the slit positioning, we cut several masks with a pattern of square holes 3 mm wide and with the usual contour. We used the LPKF machine itself to measure the aperture positions, by mounting a microscope fixed to the laser head. The mask was laid on an invar sheet secured to the working platform, and after a preliminary alignment, the procedure was to move it in small steps until the hole edges were centered under the eyepiece reticle and to read the displacements using the internal glass rules. When a mask has to be cut, the invar sheet is fixed to the working platform by means of manual clamps, and two pneumatic pistons apply an adjustable force to keep it flat. The results obtained from the measures show that the accuracy of the aperture positioning on cut masks depends mainly on the tension applied during cutting: a high force (50 kg) means an elastic elongation of the sheet that is released when the contour is cut, and smaller distances with respect to the nominal ones are systematically measured. A low force (<10 kg) is not sufficient to straighten the sheet and produces higher distance values. At the end of an optimization process, which required a long series of measurements, we adopted a tensioning force of ~ 18 kg as the best trade-off. To have a more repeatable and stable tensioning force, we have substituted the pneumatic pistons with nine mechanical springs, applying 2 kg each. The final evaluation is that a positioning accuracy $\leq 15 \mu\text{m}$ is verified.

5.3. Slit Edge Roughness

The fine tuning of the laser cutting machine was carried out by having the slit edge roughness as the driving parameter. A protocol was thus established leading to the cutting of a number of samples suitable for roughness measurements, performed using the Talysurf Plus instrument described in § 3.6. The

sample sides are scanned one at a time for thickness by the chisel edge stylus, and the roughness profiles are acquired and stored for off-line analysis. First the slope introduced by the sample nonhorizontal mounting is removed, by a linear fit, and then the rectified profile is successively filtered by two high-pass Gaussian filters. First, with a cutoff length of 0.12 mm (1 pixel of the CCD), the parameter W_q , the rms of the roughness at pixel-size scales, is computed from the filtered profile, over a scan length of 25 mm. Second, with a cutoff length of 2.5 mm, the parameter W_r , the maximum peak to valley of the edge waviness, is calculated. The samples prepared for roughness measurements must be handled and mounted under the probe very carefully because any mechanical shock makes the sample unusable; we discovered that dust and any dirt deposited on the sample border can easily mimic a bad cutting performance: thus sample measurements representative of the slit edge roughness to be found in the masks must be carried out in the same environmental conditions as mask manufacturing, i.e., in an air-conditioned, reasonably clean room. The quality control protocol was applied before and after the shipment of the MMU to Paranal. The roughness measurements obtained on nine samples in Europe and in Chile showed no significant difference. The obtained mean values are shown in Table 5, and a typical roughness meter plot is shown in Figure 8.

5.4. Scientific Implications

The results obtained not only meet the specifications, but, even more important, guarantee that observations will yield good-quality data. Thanks to the slit positioning accuracy we obtained through the choice of the mask material and the fine-tuning of the cutting operations, objects on the sky can be placed in slits all over the unvignetted Nasmyth focus covered by VIMOS, making it truly possible to obtain several hundreds of meaningful spectra of faint objects in one exposure. The excellent slit edge roughness quality guarantees optimum sky subtraction, especially of bright-sky line regions, even in the case of low signal-to-noise ratio.

6. MMU OPERATION CONCEPTS

The MMU operation concepts have been devised to provide a smooth and orderly mask flow. At least for some time since after VIMOS commissioning, preimaging is a requirement for mask design. Once the files describing a mask set have been prepared by the astronomer, they must reach the MMU so that mask production can start. Since the spectroscopic observations can be scheduled up to a few months later, masks must be identified and stored so that they can be univocally retrieved when they must be inserted in the ICs just before the observations. The instrument control software must be made aware of the IC position in which a specific mask is to be found. Furthermore, the SCs have a limited capacity, and from time to time it is necessary to discard masks which have a low probability of being used in order to leave room for new masks.

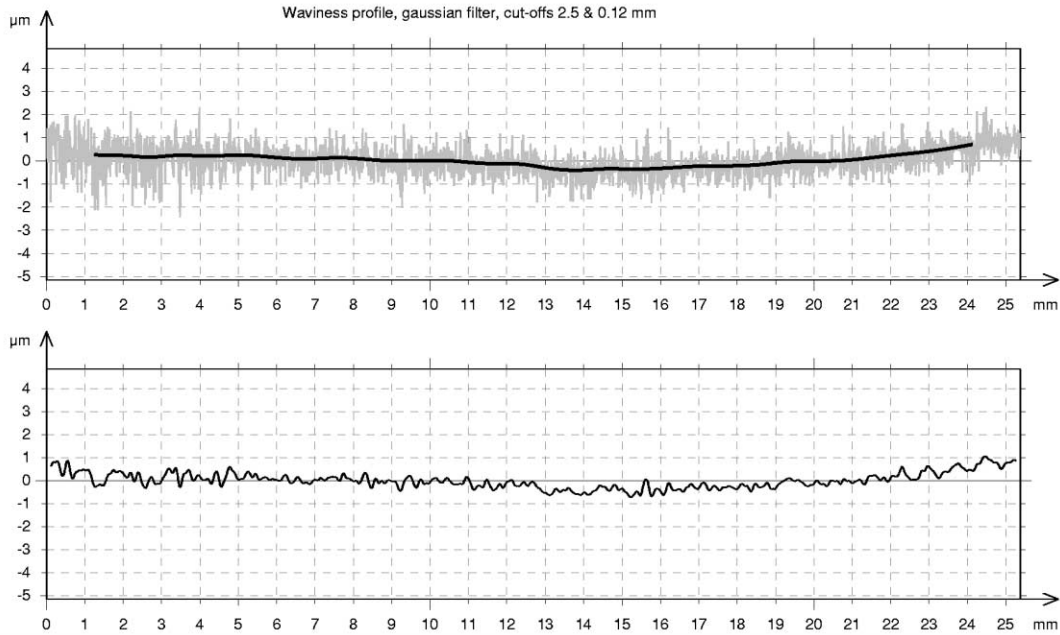


FIG. 8.—Typical roughness meter plots of a standard measurement sample. The linearized rough data are shown in gray in the top panel together with the filtered (waviness) profile using a 2.5 mm cutoff (*thick line*). This particular sample has a W_t of 1.13 μm . The bottom panel contains the profile filtered with a 0.12 mm cutoff, which gives the pixel-scale roughness. This particular sample has a W_q of 0.337 μm .

MMU routine operations will be totally slaved to orders issued by instrument software modules running on separate workstations. The only module actually talking to MMU is, in the case of VIRMOS, an instrument-specific mask conversion software (MCS module) whose purpose, besides transmitting job orders and retrieving termination reports for all activities, is also, for the mask manufacturing case, to translate the slit positions on the sky (selected by the astronomer using the mask preparation software; see Garilli et al. 1999) from pixels to millimeters with respect to the quadrant optical axis using the CCD-to-mask transformation matrix.

The purpose of the entire MMU system is to perform the following operations:

1. Manufacture the masks on the laser machine requested via a mask manufacturing job order (MMJ) and store the manufactured masks in the SCs.
2. Load the masks requested via a mask insert job order (MIJ) into the ICs.
3. Get rid of masks and related files no longer needed as requested via a mask discard job order (MDJ).
4. Manage and recover contingency conditions which may occur during the above tasks.

In all operations the MMU will recognize only masks by their individual six-digit code and will normally handle entire mask sets. A mask set is defined as a set of four masks, with the same last five digits in the code, used for the same observation in the four VIMOS or NIRMOS quadrants. All operations (except con-

tingency recovery and maintenance operations managed autonomously by the MMU operator) are executed after receipt from the MCS of a job order in the form of a file transferred into a staging area of the MHCU, and operations will terminate upon placing a termination report in the same staging area, to be retrieved by the MCS, which has also access to the tables describing the current content of the SC (SCT) and of the ICs (ICT). The SCT, for each quadrant, is a list of 100 items containing the codes of the masks currently stored or “empty,” with no information about the slot where the mask is located. The ICT, for each instrument cabinet, is a list of 15 items which combine the slot number with the code of the contained mask.

6.1. Mask Manufacturing and Storing

The information about the slit positions and sizes is contained in the machine slit files (MSF) transmitted together with an MMJ. The full manufacturing cycle is a four-step operation (Fig. 9).

1. The MHSw function *convert* selects an MMJ and converts the MSF files into the Gerber (Gerber 1997) CAD format, accepted in input by the LPFK CircuitCam software. The MSF-to-Gerber conversion takes care of items relevant for masks, such as the correction for the calibrated offsets of the optical axis with respect to the mask center and the insertion of the mask contour, fixing holes, and other control apertures (see Fig. 3) which are merged from template files and assigned to appropriate layers. This arrangement is highly modular and allows

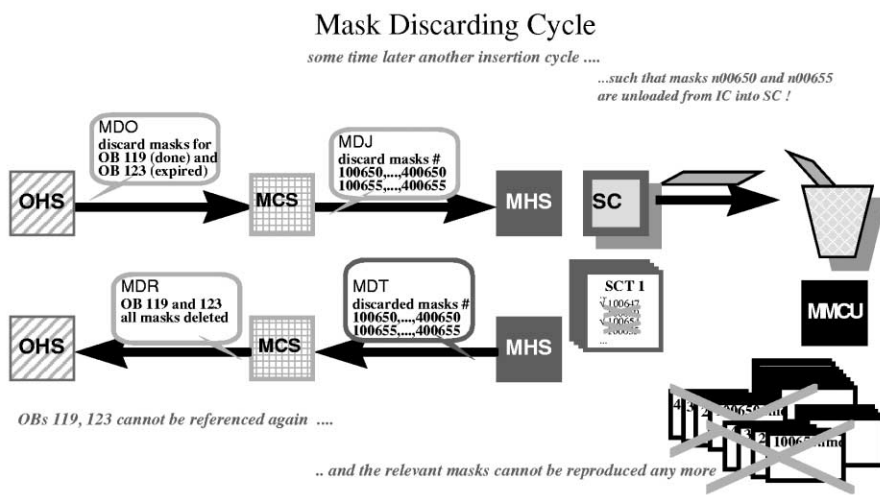
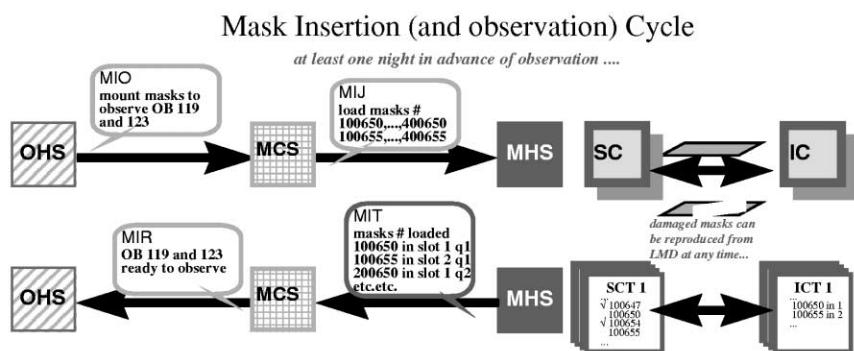
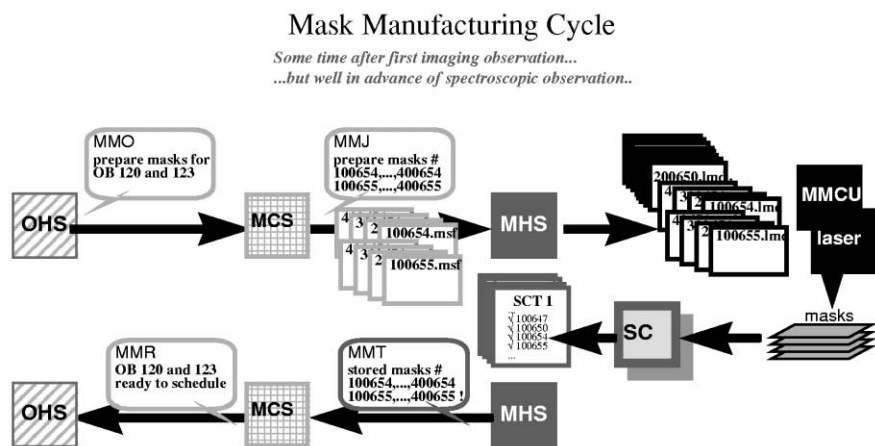


FIG. 9.—Typical mask handling flow. Hatched boxes indicate VLT/Instrument software modules (like OHS [observation handling software] and MCS [mask conversion software]), while filled boxes indicate MMU components. In the mask manufacturing cycle, from mask manufacturing orders (MMO, arranged by observing blocks [OBs]), MCS generates mask manufacturing jobs (MMJ) issued to MMU, which processes the associated files (.msf and .lmd), produces masks, stores them in the SC, updates the SC table (SCT), and prepares the MMT report from which MCS generates the final mask manufacturing report (MMR). In the mask insertion (and observation) cycle, from mask insertion orders (MIO), MCS issues MIJs to MMU, which exchanges the needed mask between SC and IC, updates the SC and IC tables, and prepares the mask insertion termination report (MIT) from which MCS generates the final mask insertion report (MIR). A mask can be discarded only once it has been used for observation or declared invalid by OHS and if it is in the SC. From mask discard orders (MDO, arranged by OBs), MCS issues MDJs to MMU, which allows one to search the masks to be discarded, gets rid of any associated file (so that the mask cannot be reproduced any more), updates the SC table, and prepares the mask discard termination report (MDT) from which MCS generates the final mask discard report (MDR).

one to tune and replace such characteristics without recompiling the code, while at the same time it keeps effectively decoupled the parameters specific to mask manufacturing from those specific to the astronomical observation.

2. LPKF CircuitCam software converts the Gerber files into proprietary format (*lmd*) files, transferred to MMCU and accepted by the StencilMaster software; at the same time it optimizes the cutting path for the laser beam and associates the layers with the cutting tools and manufacturing phases.

3. The operator places an invar sheet on the working platform of the laser machine and runs the function Cut Manager on the MMCU, which gives him access to StencilMaster to cut the mask.

4. At the same time, the operator runs the MHSw function *store* on the MHCU, which, by reading the bar code, indicates in which quadrant section of the SC the mask must be placed. Acknowledgment of these operations will automatically update the SC table and write the MMT (mask manufacturing termination report), which will eventually be retrieved by the MCS.

6.2. Instrument Cabinets Preparation

When the ICs must be loaded with a new set of masks, the operator finds an MIJ on the MHCU. The ICs coming from the telescope are inserted in the IC box which is placed on the robot, and the operator runs the *IC preparation* function of the MHSw. Loading the ICs is a two-step process: this is accomplished by running first the *unload* (sub)function, at the end of which the no longer needed masks are returned to the SC while the masks still needed are left in place; the IC and the SC tables are updated. Then the *load* (sub)function is started, which allows one to search the requested mask in the SC and to insert the masks into free IC slots, by appropriately moving the IC box. The search in the SC occurs manually, by moving the bar code scanner until the requested mask is located (the computer gives an audio signal as long as the scanner beam is located in front of the requested mask). The bar code is double-checked by the scanner located on the robot stand before inserting the mask into the IC. The SC and IC tables are updated again, and a report (MIT) is made available to MCS. The report and the updated tables are propagated to be used for mask insertion management at the instrument focal plane.

6.3. Mask Discarding

To make room in the SC for newly manufactured masks, an MDJ must be issued whenever a mask set is no longer required (the observation has been either executed or expired because of celestial constraints). The *discard* function should normally have priority with respect to any others. It allows the operator to search (as described in § 6.2) for the masks to be discarded and to remove them from the SC, thus deleting the files of the mask from the archives, updating the SC table, and issuing the final report.

6.4. Recovery Functions and Error Handling

Great care has been dedicated to manage the possible errors during mask handling (e.g., mask dropped or damaged during manual displacements, wrong insertion into the SCs or ICs, problems in bar code scanner or robot connection, etc.). All the error messages are listed in the user's manual and contain the suggested recovery procedure using the eight provided recovery functions.

7. SUMMARY

The VIRMOS mask manufacturing unit is now operational at Paranal Observatory, following verification that the specifications set at the beginning of the project have been met. The laser cutting machine has been finely tuned with an optimal choice of the parameters, and, although the MMU is largely assembled from industrial products, every effort has been made to design and implement software tools which would make the mask flow nicely fit in the VLT data flow system. The slit quality that the VIRMOS MMU provides makes it the best operational tool for multiobject spectroscopy applications.

The VIRMOS-MMU manufacturing is done under ESO contract 50979/INS/97/7569/GWI. The MMU development was aided by financial support from Italian CNR and CNA. We warmly thank LPKF technical staff (T. Nagel, A. Müller, and S. Bönigk) for their appreciated collaboration during the tuning of the laser cutting machine and N. D'Addea (CNR-ITIA) for lending us the laser interferometer system. We also thank G. Avila and the Paranal ESO Engineering staff for their help during installation of the MMU at the Observatory.

REFERENCES

- Conti, G., Chiappetti, L., Mattaini, E., Maccagani, D., Le Fèvre, O., Saisse, M., & Vettolani, G. 1999, in Conference on Telescopes, Instruments and Data Processing for Astronomy in the Year 2000, S. Agata, *Astro Tech J.*, 2, 2 (<http://www.sait.it/Astrotech/>)
- Di Biagio, B., Le Coarer, E., & Lemaitre, G. 1990, *Proc. SPIE*, 1235, 422
- Garilli, B., Bottini, D., Tresse, L., Le Fèvre, O., Saisse, M., & Vettolani, G. 1999, Conference on Telescopes, Instruments and Data Processing for Astronomy in the Year 2000, S. Agata, *Astro Tech J.*, 2, 2 (<http://www.sait.it/Astrotech/>)
- Gerber System Corporation. 1997, Gerber RS-274X Format Guide, Rev. B
- Le Fèvre, O., et al. 1998, *Proc. SPIE*, 3355, 8
- . 2000, *Proc. SPIE*, 4008, 546
- Oke, J. B., et al. 1995, *PASP*, 107, 375
- Schink, H., et al. 2000, *Proc. SPIE*, 4008, 175
- Szeto, K., Stilburn, J. R., Bond, T., Roberts, S., Sebesta, J., & Saddlemyer, L. K. 1997, *Proc. SPIE*, 2871, 1262